Redox- and anion-linked protonation sites in horseradish peroxidase: analysis of distal haem pocket mutants

Brigitte MEUNIER*, Jose Neptuno RODRIGUEZ-LOPEZ†[1], Andrew T. SMITH‡, Roger N. F. THORNELEY† and Peter R. RICH*[2]

*Glynn Laboratory of Bioenergetics, Department of Biology, University College, Gower Street, London WC1E 6BT, U.K., †Nitrogen Fixation Laboratory, John Innes Centre, Colney Lane, Norwich NR4 7UH, U.K., and ‡School of Biological Sciences, University of Sussex, Falmer, Brighton BN1 9RQ, U.K.

We have investigated the effects of mutations at residues His-42, Arg-38 and Phe-41 in the distal haem pocket of horseradish peroxidase on the changes in protonation state that accompany redox- and ligand-linked changes to the haem group. The mutations H42L and R38L result in the loss of a characteristic pH dependency in the visible spectrum of the ferrous form and a diminished dependency of the midpoint redox potential of the haem group on pH. The results support the view that His-42, with its pK probably modulated by Arg-38, provides the protonation site on the reduced enzyme that is responsible for these pH dependencies. The mutations H42L and R38L also have major effects on the binding of cyanide to the haem. We have already reported that binding of cyanide to the ferrous forms of these mutants becomes too weak to be measurable [Meunier, Rodriguez-Lopez, Smith, Thorneley and Rich (1995) Biochemistry **34**, 14687–14692]. The pH dependency of the rate constants for binding of cyanide to the oxidized form of H42L suggests that CN^- is the kinetically active species, in contrast with wild-type horseradish peroxidase, where HCN is the binding form. For the R38L variant, the pH dependency of cyanide binding suggests that the pK of His-42 in the absence of Arg-38 is raised to 7.5–8, in the oxidized form. In contrast with these changes, the mutant F41A exhibits cyanide-binding behaviour that is similar to that of the wild type, both in its oxidized and reduced forms. However, the rate constant for carbon monoxide recombination increases substantially, suggesting that the access route for carbon monoxide, but not for cyanide, is perturbed by this amino acid substitution.

INTRODUCTION

The pH dependency of the midpoint potential of horseradish peroxidase (HRP) has been well established [1]. At acid pH a redox-linked proton is bound on reduction. The pK of the ferrous enzyme of around 7.5 for this process results in pH independence of the midpoint redox potential at moderately alkaline values. At pH values above 10, further pH dependency of midpoint potential is associated with the alkaline transition [1].

The pH dependency of the dissociation constant of the cyanide compound of ferric HRP shows clearly that the stable bound species involves the net binding of HCN, rather than CN^- [2]. It has also been shown that the K_D (dissociation constant) for the reaction of cyanide with reduced HRP is independent of pH above pH 7.5 [3], again consistent with co-binding of a proton in association with the cyanide anion. Below pH 7.5, however, the K_D of the ferrous form for cyanide increases with decreasing pH [4]. We have concluded from these data that the redox-linked and the anion- (such as cyanide anion) linked protonation site(s) are mutually exclusive. This exclusivity is further corroborated by the pH independence of the midpoint redox potential of cyanide-ligated HRP [4]. These results illustrate the role of charge compensation by protonation changes in this system [5].

Two possibilities may account for the mutual exclusivity of the redox- and cyanide-linked protonations: the protons might compete for the same protonation site or, alternatively, the two sites might be structurally separate, but might interact anticooperatively so that the binding of a proton at one site lowers the pK of the other. Although there has been considerable discussion of possible protonation sites in the peroxidases, the matter appears to be unresolved. For HRP, protonation of this site is responsible for the pK_{red} (the pK of a group when the haem is reduced) of around 7.5 [1], for a small change in the recombination rate constant with CO [6], and for spectral shifts in the visible band [7], Raman [8,9], infra-red [10] and NMR [11] spectra. In the case of both HRP and cytochrome *c* peroxidase (C*c*P), the distal histidine has been proposed to provide the protonation site for the redox-linked proton [7–9,12,13]. However, the identification of this protonation site as His-42 has been challenged [14,15]. Other possibilities include Arg-38 and its associated water molecules [16], the haem propionates and their associated amino acids (as is the case for many *c*-type cytochromes that exhibit redox-linked pK shifts [17–19]), and other protonatable groups that may be influenced by the haem redox state, such as His-40. The proximal histidine itself can be ruled out as a candidate, since it is hydrogen bonded to Asp-247, and both Raman [8,9,20] and NMR [11,21] data show that it does not change its protonation state with pH.

In the case of C*c*P, the situation is more complex, since it has been shown that analogous changes at roughly the same pK values are associated with a concerted two-proton exchange [22,23]. One of the protonation sites has been identified by site-directed mutagenesis as His-181, a residue that is hydrogen bonded to a haem propionate [24]. This histidine is not conserved in HRP [25]. The situation regarding the site of anion-linked protonation is clearer. Crystal-structure studies of the cyanide and fluoride complexes of oxidized C*c*P show hydrogen bonding

Abbreviations used: HRP, horseradish peroxidase; C*c*P, cytochrome *c* peroxidase; K_D, dissociation constant; k_{on} and k_{off}, on and off rate constants; pK_{ox} or pK_{red}, pK of a group when the haem is oxidized or reduced respectively; k_{obs}, observed rate constant.

[1] Present address: Department of Biochemistry and Molecular Biology, School of Biology, University of Murcia, Spain

[2] To whom correspondence should be addressed.

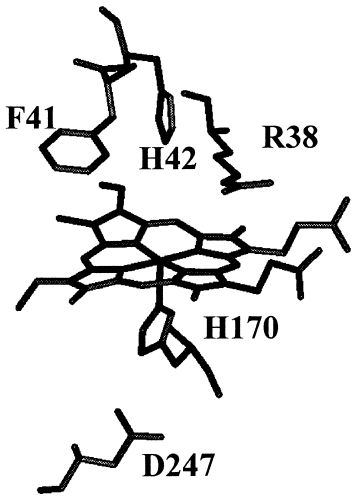

Figure 1 Key residues in the haem pocket of HRP

The structure has been drawn from the co-ordinates of the peanut peroxidase published by Schuller et al. [34]. Numbering of the residues is according to the HRP sequence.

to, and therefore protonation of, the distal histidine residue [26,27]. This conclusion is corroborated for the cyanide complex of ferric HRP by studies of its Raman [8,9], infra-red [28] and NMR [11] properties.

Although a high-resolution structure of HRP is not yet available, the structure around the haem can be predicted [29,30] based on homology with other peroxidases [31], such as C*c*P [32], lignin peroxidase [33] and peanut peroxidase [34], whose atomic structures have been determined. Site-directed mutations of the key catalytic residues in HRP are available and can be used to probe the roles of residues in the movement of protons associated with redox and ligand changes. Some of the effects of mutations of the distal haem-pocket residues His-42, Arg-38 and Phe-41 (Figure 1) have been already studied [35–38]. The rates of guaiacol oxidation were lowered by factors of 10^5 and 30, whereas this rate was not affected in F41L [35,36]. Similarly, in H42L and R38L the rates of compound I formation were lowered by 10^6 and 10^3 respectively, and compound II was not observed [35,36], whereas there was little effect of an F41A mutation on these parameters [35]. In the present work, we have investigated the effects of mutations of these residues on the protonation state accompanying redox and ligand changes in order to investigate further the identity of the redox- and anion-linked site(s) of protonation.

MATERIALS AND METHODS

Preparation of peroxidase

Production of wild-type and mutant forms of recombinant HRP (EC 1.11.1.7) isozyme C has been described in [16,38]. A PCR-based technique with the HRPC synthetic gene [39] as template was used to generate insert DNA with the required mutations. Amplified DNA fragments bearing the mutation were cloned in frame into the wild-type gene in the HRP expression vector pAS5 [38]. Growth and induction of *Escherichia coli* strains producing recombinant peroxidase variants and folding and activation of recombinant HRP were performed as described previously [38,39].

Optical measurements

Difference spectra and transient kinetics at individual wavelengths were monitored with a single-beam scanning/kinetic instrument built in-house (Glynn Research Enterprises, Bodmin, U.K.). Short actinic light pulses (10 ns halfpeak width, 532 nm, >100 mJ/pulse) were provided by a frequency-doubled Nd-YAG laser (Spectron, Rugby, U.K.). Transients were detected with a photomultiplier protected by appropriate combinations of filters. Photolysis transients were recorded individually at several wavelengths.

Reduction of cyanide-ligated HRP by the photogenerated radical of deazaflavin

We have already shown that dithionite is inadequate as a reductant to generate the cyanide adduct of ferrous HRP at low pH [4]. Instead, ferric HRP was dissolved to a final concentration of 2 μM in 0.5 ml of 0.2 M potassium phosphate containing [40] 15 μM deazaflavin as a photoreductant (7,8-nor-3-methyl-5-deazalumiflavin, kindly supplied by Dr V. Massey, University of Michigan, Ann Arbor, MI, U.S.A.) and 10 mM EDTA. The EDTA acted as an efficient electron donor to the photoexcited flavin and did not cause detectable unfolding of the HRP on the timescale of these experiments. Anaerobiosis was obtained by addition of 10 mM glucose/100 units/ml glucose oxidase/500 units/ml catalase. Neutralized potassium cyanide was added, and the mixture was kept anaerobic with a positive pressure of argon above the liquid surface. The cyanide-ligated HRP was reduced by the deazaflavin radical [40], generated by 10–20 s illumination with white light from a standard projector lamp. Full formation of the reduced cyanide-ligated enzyme was established by monitoring the Soret band changes.

Potentiometric titrations

Anaerobic redox titrations were carried out in 2.5 ml of 0.1 M potassium phosphate at different pH values. HRP was added to a final concentration of around 2 μM. The buffer was kept anaerobic with a positive pressure of argon above the liquid surface. Redox mediators were (midpoint potential in mV, concentration in μM): 2-hydroxy-1,4-naphthoquinone (-220, 10), anthraquinone-2,6-disulphonate (-184, 10), anthraquinone-2-sulphonate (-250, 10), benzyl viologen (-311, 10) and methyl viologen (-455, 10). Sodium dithionite (50 mM) and 10 mM ferricyanide were used as reductant and oxidant respectively. Redox potentials were measured in stirred samples with a platinum electrode and an Ag/AgCl reference electrode. For each measurement, stirring was stopped and spectra were taken from 390 to 460 nm. The potential was recorded at the start and the end of the scans, and absorbency changes were plotted againstthe average of the two potential readings. Haem reduction was monitored by a triple wavelength measurement at $\{\Delta A_{440} - [(\Delta A_{430} + \Delta A_{450})/2]\}$. The triple wavelength measurements minimized interference from redox dyes or baseline drifts.

RESULTS

pH dependency of the static spectra of the ferrous forms

It is well known that the visible spectrum of unligated ferrous HRP shows a small change in response to pH with a characteristic pK of 7.4 [7,41]. This is illustrated for the wild-type enzyme in

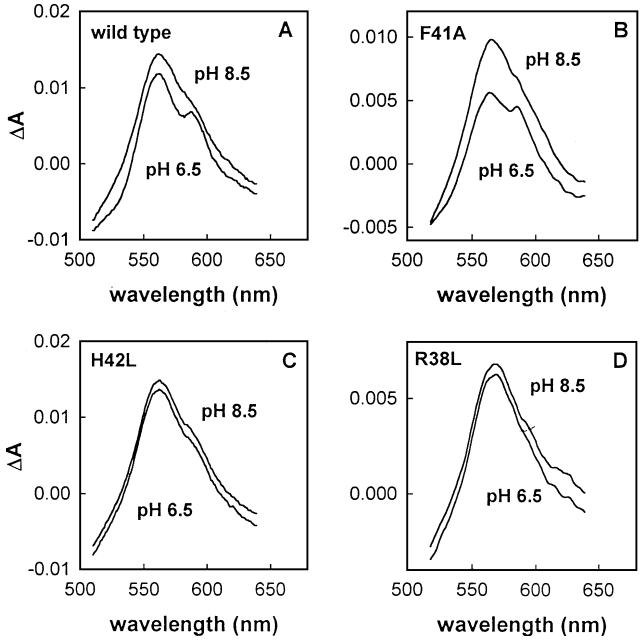

Figure 2 pH dependency of the static spectrum of ferrous enzymes

The enzymes were dissolved to a concentration of 2–3 μM in 0.5 ml of 0.1 M potassium phosphate at pH 6.5 and 8.5 and reduced with solid sodium dithionite. The Figure shows the reduced-minus-oxidized difference spectra of the wild-type enzyme (**A**), F41A (**B**), H42L (**C**) and R38L (**D**).

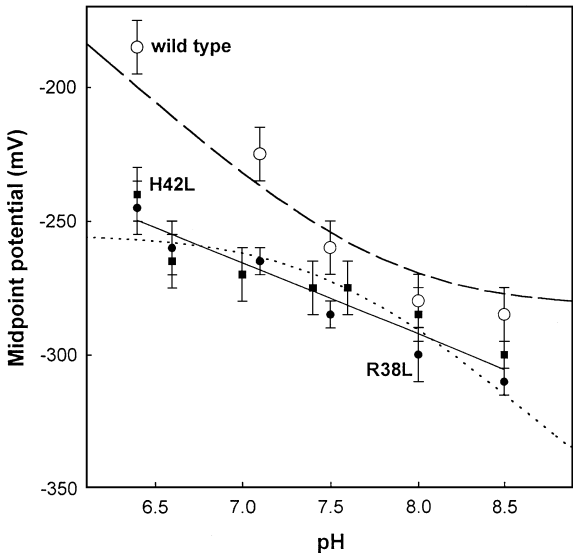

Figure 3 pH dependencies of midpoint potentials

○, Wild type; ■, H42L; ●, R38L. Anaerobic redox titrations were performed as described in the Materials and methods section. The dashed and dotted lines represent simulations of the midpoint potential versus pH for an $n = 1$ protonation with pK_{red} and pK_{ox} of 7.8 and 4.5 for the wild type (dashes) and 10 and 7.5 for the mutants (dots) (see the text). For comparison (see the text) a straight line (solid line) with a slope of -25 mV/pH is also shown.

Figure 2(A), where reduced-minus-oxidized difference spectra are compared for pH values of 6.5 and 8.5. Analogous spectra taken with the F41A mutant (Figure 2B) show a similar pH dependency. In contrast, the visible reduced-minus-oxidized difference spectra of the H42L and R38L mutants were essentially unchanged between these pH values (Figures 2C and 2D) and even down to pH 5.5 (results not shown).

pH dependency of midpoint potentials

The pH dependency of the midpoint potential of recombinant wild-type HRP is essentially the same as that reported for native HRP [1]. At low pH, a slope of around -60 mV/pH unit was observed, until a pK above 7 was reached and the redox potential became pH independent. In Figure 3, the simulated curve (dashed line) has been obtained with a pK_{red} of 7.8. This classical behaviour [42] is caused by a redox-linked protonation site whose pK is $\leqslant 5$ when the haem group is oxidized and is around 7.8 when the haem group is reduced.

The potentiometric behaviour of the H42L and R38L mutant enzymes as a function of pH is also shown in Figure 3. In both cases, the redox potentials were shifted to lower values, and the pH dependencies of the midpoint potentials at low pH were weaker than that of the wild-type form. Because of the limited range of pH values that could be used with these enzymes, there is no unique model to explain this behaviour. It is possible to overlay a simulation for a redox-linked protonation with pK_{ox} (the pK of a group when the haem is oxidized) and pK_{red} of 7.5 and 10 respectively (Figure 3, dotted line). However, the data could be equally fitted with a fixed weak pH dependency over the whole range of around -25 mV/pH unit (solid line).

pH dependency of ligand binding

Cyanide binding to oxidized enzymes

Cyanide binding to oxidized forms of HRP was monitored kinetically by following the characteristic shift in the Soret band on ligand binding at 426–400 nm. Plots of the observed rate constants (k_{obs}) increased linearly with increasing cyanide concentrations, and values for k_{on}, k_{off} and K_D can be determined from their slopes and intercepts. The pH dependencies of k_{on}, k_{off} and K_D were determined by repeating such measurements at different pH values [43] and are summarized in Figure 4.

As expected for the wild-type form, all three parameters are pH independent between pH 5.5 and 8.5, consistent with the net binding of HCN to a protein in which there is no associated protonatable group with a pK in this range [2]. A similar pH independence of these parameters was also found for the mutant form F41A (results not shown).

In contrast, the mutations H42L and R38L have major effects on the parameters for cyanide binding. For both mutants, the binding and dissociation rate constants, k_{on} and k_{off}, were lower than those of the wild type. At pH 6.5, the k_{on} values estimated for the wild type, H42L and R38L were $(75 \pm 5) \times 10^3$, 8.5 ± 1 and 75 ± 10 s^{-1} respectively. Furthermore, clear pH dependencies were observed. For H42L, the plot of $\log k_{on}$ against pH (Figure 4A) gave a straight line with a slope close to 1. The behaviour of R38L was different. As shown in Figure 4(B), between pH 6.5 and 8.5, the k_{on} increased sharply with increasing pH, and the plot of k_{on} against pH could be simulated by a curve obtained for an $n = 1$ protonation with a pK of 7.9. Consistent with this simulation, the plot of $\log k_{on}$ against pH had a slope of around 1 below pH 8.

The dissociation rate constants are also slower in both mutants (Figure 4C). At pH 6.5, the k_{off} estimated for the wild type, H42L and R38L were 0.15 ± 0.05, $(0.6 \pm 0.3) \times 10^{-3}$ and

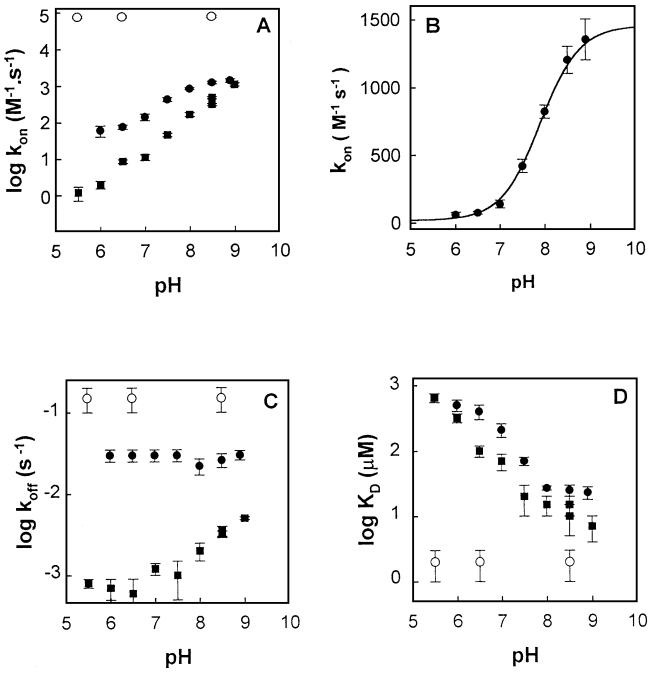

Figure 4 pH dependencies of the rate constants of cyanide binding to the oxidized forms

○, Wild type; ■, H42L; ●, R38L. The enzymes were dissolved in 0.5 ml of 0.1 M potassium phosphate (pH 5.5–8.5) or 0.1 M Tris/HCl (pH 9), to a final concentration of 1 μM. Successive additions of neutralized KCN were made, and the optical changes due to formation of the cyanide compound were monitored at 426–400 nm. At each cyanide concentration, k_{obs} values were obtained by fitting exponential decays and were plotted against cyanide concentrations. The *y*-axis intercept of such plots is a measure of k_{off}, the slope is a measure of k_{on}, and K_D is k_{off}/k_{on}. These derived values are plotted as logk_{on} (**A**), logk_{off} (**C**) and logK_D (**D**) against pH. (**B**) k_{on} for R38L against pH.

Table 1 Kinetics of CO and cyanide recombination to reduced HRP after flash photolysis

Enzymes were dissolved in 0.5 ml of 0.1 M potassium phosphate at pH 8.5 to a concentration of 0.8 μM and were reduced with sodium dithionite. The CO adduct was formed by bubbling with CO until saturated. Cyanide-ligated enzyme was formed by addition of 1–40 mM neutralized KCN. Extents of formation of the reduced CO- and cyanide-ligated states were confirmed by monitoring Soret band changes. Single laser-induced transients were recorded at 423 and 443 nm for CO and 432 and 448 nm for cyanide. k_{obs} values were obtained by fitting exponential decays to the transients. In the case of the cyanide recombination kinetics, k_{obs} values were plotted against cyanide concentrations and k_{on}, k_{off} and K_D were estimated from this plot in the same manner as that described for the data in Figure 4. The CO and cyanide recombination kinetics were slightly biphasic with 10–20% slow phase, and the CO recombination kinetics trace of R38L showed an additional faster phase at higher pH values (see the text). We present here only the k_{obs} for the major phase of each sample. –, not done.

	CO recombination	Cyanide recombination		
	k_{obs} (s^{-1})	k_{on} ($M^{-1}\cdot s^{-1}$)	k_{off} (s^{-1})	K_D (mM)
Wild type	4.4	90 ± 5	0.09 ± 0.02	0.9 ± 0.2
H42L	35	–	–	> 200
R38L	120	–	–	> 200
F41A	1600	60 ± 3	0.06 ± 0.01	1 ± 0.2

$(0.3 \pm 0.05) \times 10^{-1}$ s^{-1} respectively, and little pH dependency was observed.

The pH dependencies of the dissociation constants are shown in Figure 4(D). At pH 8.5, the K_D values estimated for the wild type, H42L and R38L were 2 ± 1, 10 ± 5 and 25 ± 5 μM. In contrast with the pH-independent wild-type value, for H42L the plot of log K_D against pH gave a straight line with a slope of around 1, at least below pH 8. With R38L, the K_D was pH dependent below pH 8 but became pH independent above this pH.

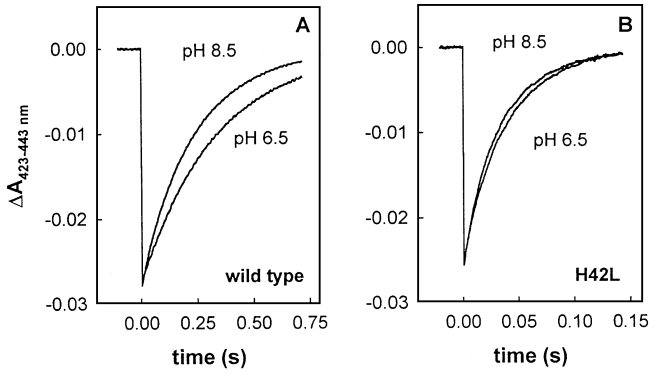

Figure 5 pH dependency of CO recombination kinetics after flash photolysis

Enzymes were dissolved at room temperature in 0.5 ml of 0.1 M potassium phosphate at pH 8.5 or 6.5 to a concentration of 0.8 μM. Samples were reduced with sodium dithionite and saturated with CO by bubbling. Laser-induced transients were recorded at 423 and 443 nm.

CO binding to reduced enzymes

The room-temperature recombination of CO after photolysis was monitored at saturating (1 mM) CO concentration. Exponential decays were fitted to the kinetic transients at pH 8.5, and the observed recombination rate constants (k_{obs}) are presented in Table 1. All three mutant enzymes had faster recombination rates. This increase was most marked with the F41A mutant.

It is already known that the rate of recombination of CO shows a small pH dependency [6]. This is shown in Figure 5(A). For the wild type, the k_{obs} values at pH 6.5 and pH 8.5 were estimated to be 3.5 s^{-1} and 4.4 s^{-1} respectively. This behaviour was therefore examined in the mutant proteins. The pH dependency of the rate constant was lost in the H42L mutant (Figure 5B). In the case of R38L, the 120 s^{-1} kinetic phase also appeared to remain pH independent (results not shown). However, measurements with this mutant were complicated by an increasing biphasicity of the kinetics with increasing pH. In this case, a fast phase of around 400 s^{-1} progressively appeared with increasing pH and at pH 8.5 represented 27% of the transient change. This fast phase was even more prominent in the presence of EDTA, accounting for the higher k_{obs} that we have reported previously with this mutant [16].

Cyanide binding to reduced enzymes

The kinetics parameters of cyanide binding to the reduced enzymes at pH 8.5 are presented in Table 1. The behaviour of the wild-type enzyme has been described previously [3,4]. Cyanide binding is pH independent above pH 7.5. Below pH 7.5, the K_D increases and k_{on} and k_{off} decrease with decreasing pH.

In the case of the mutants H42L and R38L, we were unable to measure any significant binding of cyanide at cyanide concentrations up to 10 mM, indicating that the K_D values had risen above 100 mM [16]. In contrast, the kinetics of cyanide binding

to the reduced form of F41A at pH 8.5 were essentially identical with that of the wild type, as was the K_D value of 1 mM. As is also the case with the wild-type form, the affinity for cyanide became weaker at acid pH. By using the photogenerated radical of a deazaflavin [40] to reduce the enzyme at low pH in the presence of cyanide [4], the K_D at pH 6.5 was estimated to be 10–30 mM, a value that we could not obtain more accurately because of the instability of the enzyme at the high concentrations of cyanide required for binding. Despite this uncertainty, it is clear that cyanide binding to the F41A mutant is very similar to the cyanide-binding behaviour of the wild-type form.

DISCUSSION

The protonation site responsible for pH dependencies of midpoint potentials, static spectra and CO recombination kinetics

The pH dependency of the midpoint potential of HRP has shown that at acid pH a redox-linked proton is bound on reduction. The pK of the ferrous enzyme of around 7.5 for this protonation results in pH independence at more alkaline values [1]. Protonation of this same site could be responsible for spectral shifts in the visible band [7] and for the small change in the rate constant for CO recombination [6]. Binding of CO shifts the pK of the site to 8.8, as judged from the pH dependency of the infrared stretch frequency of the bound CO [10].

The distal histidine has been proposed to provide the redox-linked protonation site [7–9,12,44], and it is reasonable therefore to expect that it is responsible for the other pH-dependent effects. However, the identity of this protonation site with His-42 has been challenged. For example, a study of the pH dependency of the FTIR spectra of CO-ligated wild-type HRP has suggested that Arg-38 and not His-42 was involved in hydrogen bonding [14]. In C*c*P, the pH dependencies of the optical spectra of the ferrous enzyme, of the CO-binding rates and of the midpoint potential showed a concerted two-proton change with a pK of around 7.5 [22,23]. One of the protonation sites has been identified by site-directed mutagenesis as His-181, a residue that is hydrogen bonded to a haem propionate but is not conserved in HRP. Since the mutation of the distal histidine H52L did not seem to alter the two-proton titration, the authors suggested that His-52 was not one of the protonable groups [15].

We have shown that both the H42L and the R38L mutants of HRP have weakened pH dependencies of their midpoint potentials, that they lack pH dependency of the optical spectra of the ferrous form between pH 6.5 and 8.5 and that they have lost the pH dependency of the rate of recombination of CO. These altered pH dependencies strongly support the proposal that it is indeed the same site that provides the protonation site for all of these effects with a pK_{red} of around 7.5 in the unligated ferrous form and are consistent with the view that it is His-42 that provides the site. It has been proposed that His-42 and Arg-38 act in a concerted manner in the catalytic reaction [32,45] and are hydrogen bonded to each other in the high-resolution crystal structure of the ferric form of C*c*P [32]. This interaction should modulate the pK of His-42 [19], lowering it in both the ferric and ferrous forms of the enzyme. Hence, the effects of the mutation R38L on the pH dependencies presumably arise from the disruption of this interaction so that the pK of His-42 is raised. We have observed a similar effect on the reaction of R38L with hydrogen peroxide: the pK for the formation of compound I has been estimated to be 7.5 in this mutant enzyme (J. N. Rodriguez-Lopez, J. Hernandez-Ruiz and R. N. F. Thorneley, unpublished work) and around 4 in the wild type [46,47]. These data confirm the role of Arg-38 in modulating the pK of His-42 in the ferric HRP.

The weak pH dependencies of the midpoint potentials of the H42L and R38L mutants could be simulated assuming a redox-linked protonation site with pK_{ox} and pK_{red} of 7.5 and 10 respectively (Figure 3). This is a reasonable model for the R38L mutant, since the protonation site is still present, but its pK is no longer shifted downwards by its interaction with arginine. In the H42L mutant, however, the protonation site for the redox proton is lost altogether, so that the residual weak pH dependency of the midpoint potential indicates that redox changes can still be charge compensated to some extent by binding of protons to other sites, even when the major protonation site has been removed. In this case, the weak pH dependency might arise from small redox-linked pK changes of a number of groups, possibly those around the haem propionate residues. Such weak redox linkage of a number of protonation sites, leading to weak pH dependency over a wide pH range, has been observed in a variety of protein-bound redox systems, for example in some cytochrome *b* systems [48,49] and in the Q_B site of the bacterial reaction centre [50,51].

Protonation associated with anion binding

Binding of cyanide to ferric HRP

The binding of cyanide to the ferric wild-type form of HRP has been studied in detail [2]. Essentially, the data exhibited only a very weak pH dependency of the observed binding rate constant and dissociation constant between pH 5 and 8, as also shown in Figure 4. We take this to indicate that HCN is the reactive species and that the proton of HCN is co-bound in the final stable adduct. Below pH 5, the observed rate constant of binding decreases and the dissociation constant increases [2]. We interpret this as an increasing protonation of His-42 in the unligated enzyme as the pH is lowered below pH 5 so that less of the active (deprotonated) protein is available for reaction with HCN. This interpretation is in line with the conclusions from proton NMR data of the cyanide adduct of ferric HRP [11], which demonstrated that the distal His-42, which is normally in the neutral imidazole state above pH 5 in the ferric enzyme, remains as the protonated imidazolium in the cyanide-ligated ferric state over the pH range 4–11.

The rate constants for the binding of cyanide to the H42L and R38L were much lower than those of the wild type and were clearly pH dependent. For H42L, a plot of $\log k_{on}$ against pH (Figure 4A) gave a straight line with a slope of around 1 and a plot of $\log K_D$ against pH gave a slope of around -1, suggesting that the major active binding species, and the net species bound, is CN^- over the whole pH range tested. This is expected if His-42 is the site that binds the anion-associated proton in the wild-type form. Presumably, the groups that are weakly redox linked to produce a weak pH dependency of midpoint potential in this mutant (see above) are physically separated from the cyanide site and unable to influence significantly its binding parameters.

The behaviour of the R38L mutant was somewhat different. As shown in Figure 4(B), a plot of k_{on} against pH could be simulated by a single protonation site with a pK of 7.9. This again is consistent with the role of His-42 in binding of the anion-linked proton, and with a shift in its pK in this mutant to 7.5–8, as also observed by redox titration (Figure 3). Hence, the most active (deprotonated) binding form of the protein is titrated out with a pK of 7.9, leading to a pH dependency of the binding rate constant of cyanide below this pH (instead of below pH 5 as seen in the wild-type form). The pH dependency of the K_D is consistent with this analysis: above pH 7.9, the K_D becomes pH independent because a proton can bind with the cyanide anion, whereas below pH 7.9 the His-42 is protonated and no longer able to co-bind a

proton, so that the K_D increases with decreasing pH (as in the wild-type form below pH 5 [2]).

Binding of cyanide to ferrous HRP

We have shown previously that cyanide binding to the ferrous forms of the H42L and R38L mutants is very much weakened, with K_D values greater than 100 mM. This contrasts with the wild-type form, which has a K_D of 1 mM above a pH of 7.5. We had previously considered that two protonation sites might be available in the distal haem pocket, one for the redox-linked proton and a second one for the anion-linked proton [16]. However, we later showed that two simultaneous protonations do not occur, so that cyanide binding becomes weaker at pH values below pH 7.5, since the protonation site is already occupied by redox-linked protonation [4]. Hence, the reason for weakened binding of cyanide in the ferrous forms of the mutants is that the protonation site is absent altogether in H42L or is always protonated in R38L (where we estimated a pK of around 10).

Other mutations at the His-42 and Arg-38 positions

We have examined some properties of two other mutant forms, namely H42D and R38S (results not shown). Both mutants have lost the pH dependency of the static spectra of the ferrous forms. Furthermore, binding of cyanide to the ferric enzymes showed a higher K_D and was clearly pH dependent. These preliminary measurements indicate that effects of the mutations that we have studied in more detail are likely to be representative of mutations at these positions more generally, and lend support to the interpretation in terms of the importance of the His-42 and Arg-38 positions in the protonation linked with redox or ligand change.

Mutation of the distal phenylanine

The F41A and F41L mutants have been extensively studied by P. Ortiz de Montellano [34,52] and found to have enhanced oxygen-transfer properties in terms of increased rates of thioanisole sulphoxidation. In both published [38] and unpublished work (D. J. Gilfoyle and A. T. Smith, unpublished work), it has been shown that relatively small peroxidase substrates, e.g. *p*-amino-benzoic acid and aniline, are oxidized more rapidly by these mutants. In the crystal structure of peanut peroxidase [34] and of HRP [53], F41 is at the end of helix B and its C_α position is stabilized by the disulphide bond between C44 and C49 and by the distal calcium-binding site that is liganded by D43. Hence, a smaller side chain at this position is expected simply to enlarge the distal haem pocket. Indeed, the pK_a of the alkaline transition is not significantly affected in these mutants, and the pattern of NOE connectivities seen in the F41V mutant is identical with the WT [54], both suggesting that no major rearrangement of the distal pocket has occurred.

The F41A mutant form showed a pH dependency of the optical spectrum of the unligated ferrous enzyme that was similar to that of the wild-type enzyme, and also showed similar values and pH dependencies of rate constants and dissociation constants for the binding of cyanide to the ferric and ferrous states. This indicates that the protonation properties of His-42 were not affected significantly. In contrast, a major effect on the kinetics of binding of CO was observed in this mutant, with a rate of CO recombination after photolysis 360-fold faster than in the wild type. This rate is still much slower than the rate of geminate processes, which occur in a picosecond timescale at room temperature [55]. Since binding of neutral CO to the ferrous HRP occurs with no net protonation change, it seems likely that the effect on the binding rate constant is caused by effects on the pathway of CO into the distal haem pocket, suggesting that there is a route through the protein structure for CO involving the Phe-41 position. The fact that binding of the more polar cyanide is unaffected by this change may indicate that a different route(s) is taken.

This work was funded by an EC fellowship award to B.M. (BIO2-CT-94-8197), by an EPSRC research grant to P.R.R. (Grant GR/J28148) and by a grant from the EC Human Capital and Mobility Programme 'Peroxidases in Agriculture and the Environment' (ERB CHRX-CT92-0012) award to J.N.R.-L., R.N. F.T and A.T.S.

REFERENCES

1 Harbury, H. A. (1957) J. Biol. Chem. **225**, 1009–1024
2 Ellis, W. D. and Dunford, H. B. (1968) Biochemistry **7**, 2054–2062
3 Phelps, C., Antonini, E. and Brunori, M. (1971) Biochem. J. **122**, 79–87
4 Meunier, B. and Rich, P. R. (1997) Biochim. Biophys. Acta **1318**, 235–245
5 Rich, P. R. (1996) in Protein Electron Transfer (Bendall, D. S., ed.), pp. 217–248, BIOS Scientific Publishers, Oxford
6 Coletta, M., Ascoli, F., Brunori, M. and Traylor, T. G. (1986) J. Biol. Chem. **261**, 9811–9814
7 Yamazaki, I., Araiso, T., Hayashi, Y., Yamada, H. and Makino, R. (1978) Adv. Biophys. **11**, 249–281
8 Kitagawa, T. and Teraoka, J. (1982) in The Biological Chemistry of Iron (Dunford, H. B., Dolphin, D., Raymond, K. N. and Sieker, L., eds.), pp. 375–389, D. Reidel Publishing Company, Dordrecht
9 Teraoka, J. and Kitagawa, T. (1981) J. Biol. Chem. **256**, 3969–3977
10 Barlow, C. H., Ohlsson, P.-I. and Paul, K.-G. (1976) Biochemistry **15**, 2225–2229
11 Thanabal, V., De Ropp, J. S. and La Mar, G. N. (1988) J. Am. Chem. Soc. **110**, 3027–3035
12 Teraoka, J. and Kitagawa, T. (1980) Biochem. Biophys. Res. Commun. **93**, 694–700
13 Moore, G. R., Pettigrew, G. W. and Rogers, N. K. (1986) Proc. Natl. Acad. Sci. U.S.A. **83**, 4998–4999
14 Holzbaur, I. E., English, A. M. and Ismail, A. A. (1996) J. Am. Chem. Soc. **118**, 3354–3359
15 Smulevich, G., Miller, M. A., Kraut, J. and Spiro, T. G. (1991) Biochemistry **30**, 9546–9558
16 Meunier, B., Rodriguez-Lopez, J. N., Smith, A. T., Thorneley, R. N. F. and Rich, P. R. (1995) Biochemistry **34**, 14687–14692
17 Gao, Y., McClendon, G., Pielak, G. J. and Williams, R. J. P. (1992) Eur. J. Biochem. **204**, 337–352
18 Williams, R. J. P. (1991) Biochim. Biophys. Acta **1058**, 71–74
19 Moore, G. R. and Pettigrew, G. W. (1990) in Cytochromes *c*: Evolutionary, Structural and Physicochemical Aspects, pp. 309–362, Springer-Verlag, Berlin
20 Al-Mustafa, J. and Kincaid, J. R. (1994) Biochemistry **33**, 2191–2197
21 La Mar, G. N., De Ropp, J. S., Chacko, V. P., Satterlee, J. D. and Erman, J. E. (1982) Biochim. Biophys. Acta **708**, 317–325
22 Iizuka, T., Makino, R., Ishimura, Y. and Yonetani, T. (1985) J. Biol. Chem. **260**, 1407–1412
23 Conroy, C. W., Tyma, P., Daum, P. H. and Erman, J. E. (1978) Biochim. Biophys. Acta **537**, 62–69
24 Miller, M. A., Mauro, J. M., Smulevich, G., Coletta, M., Kraut, J. and Traylor, T. G. (1990) Biochemistry **29**, 9978–9988
25 Welinder, K. G., Bjornholm, B. and Dunford, H. B. (1995) Biochem. Soc. Trans. **23**, 257–262
26 Edwards, S. L. and Poulos, T. L. (1990) J. Biol. Chem. **265**, 2588–2595
27 Edwards, S. L., Xuong, N. H., Hamlin, R. C. and Kraut, J. (1987) Biochemistry **26**, 1503–1511
28 Yoshikawa, S., O'Keefe, D. H. and Caughey, W. S. (1985) J. Biol. Chem. **260**, 3518–3528
29 Smith, A. T., Du, P. and Loew, G. H. (1995) Nuclear Magnetic Resonance of Paramagnetic Macromolecules (La Mar, G. N., ed.), pp. 75–93, Kluwer Academic Publisher, Dordrecht
30 Zhao, D. Q., Gilfoyle, D. J., Smith, A. T. and Loew, G. H. (1996) Proteins **26**, 204–216
31 Welinder, K. G. (1992) Curr. Opin. Struct. Biol **2**, 388–394
32 Finzel, B. C., Poulos, T. L. and Kraut, J. (1984) J. Biol. Chem. **259**, 13027–13036
33 Edwards, S. L., Raag, R., Wariishi, H., Gold, M. H. and Poulos, T. L. (1993) Proc. Natl. Acad. Sci. U.S.A. **90**, 750–754
34 Schuller, D. J., Ban, N., Vanhuystee, R. B., McPerson, A. and Poulos, T. L. (1996) Structure **4**, 311–321

35 Newmyer, S. L. and Ortiz de Montellano, P. R. (1995) J. Biol. Chem. **270**, 19430–19438
36 Rodriguez-Lopez, J. N., Smith, A. T. and Thorneley, R. N. F. (1996) J. Biol. Chem. **271**, 4023–4030
37 Rodriguez-Lopez, J. N., Smith, A. T. and Thorneley, R. N. F. (1997) J. Biol. Chem. **272**, 389–395
38 Smith, A. T., Sanders, S. A., Thorneley, R. N. F., Burke, J. F. and Bray, R. R. C. (1992) Eur. J. Biochem. **207**, 507–519
39 Smith, A. T., Santama, N., Darcey, S., Edwards, M., Bray, R. C., Thorneley, R. N. F. and Burke, J. F. (1990) J. Biol. Chem. **265**, 13335–13343
40 Massey, V. and Hemmerich, P. (1977) J. Biol. Chem. **252**, 5612–5614
41 Yamada, H. and Yamazaki, I. (1974) Arch. Biochem. Biophys. **165**, 728–738
42 Clark, W. M. (1960) Oxidation–Reduction Potentials of Organic Systems, pp. 248–272, Bailliere, Tindall and Cox, London
43 Mitchell, R. and Rich, P. R. (1994) Biochem. Soc. Trans. **22**, 705–709
44 Doster, W., Bowne, S. F., Frauenfelder, H., Reinisch, L. and Shyamsunder, E. (1987) J. Mol. Biol. **194**, 299–312
45 Poulos, T. L. and Kraut, J. (1980) J. Biol. Chem. **255**, 8199–8205
46 Marquez, L. A., Huang, J. T. and Dunfort, H. B. (1994) Biochemistry **33**, 1447–1454
47 Araiso, T. and Dunfort, H. B. (1980) Biochem. Biophys. Res. Commun. **94**, 1177–1182
48 Rich, P. R. and Bendall, D. S. (1980) Biochim. Biophys. Acta **591**, 153–161
49 Dutton, P. L. and Wilson, D. F. (1974) Biochim. Biophys. Acta **346**, 165–212
50 Maróti, P. and Wraight, C. A. (1988) Biochim. Biophys. Acta **934**, 314–328
51 McPherson, P. H., Okamura, M. Y. and Feher, G. (1988) Biochim. Biophys. Acta **934**, 348–368
52 Ozaki, S. I. and Ortiz de Montellano, P. R. (1995) J. Am. Chem. Soc. **117**, 7056–7064
53 Gajkede, M., Schuller, D. J., Henricksen, A., Smith, A. T. and Poulos, T. L. (1997) Nat. Struct. Biol. **4**, 1032–1038
54 Veitch, N. C., Williams, R. J. P., Bray, R. C., Burke, J. F., Sanders, S. A., Thorneley, R. N. F. and Smith, A. T. (1992) Eur. J. Biochem. **207**, 521–531
55 Berinstain, A. B., English, A. M., Hill, B. C. and Sharma, D. (1990) J. Am. Chem. Soc. **112**, 9649–9650

Received 24 June 1997/26 September 1997; accepted 29 October 1997